Journal of Colloid and Interface Science 583 (2021) 563–570

Contents lists available at ScienceDirect

Journal of Colloid and Interface Science

journal homepage: www.elsevier.com/locate/jcis

Regular Article

Analyzing microalgal biofilm structures formed under different light conditions by evaluating cell–cell interactions

Hao Yuan [a], Yi Wang [a], Zhijian Lai [b], Xinru Zhang [a,c,*], Zeyi Jiang [a,d], Xinxin Zhang [a,d]

[a] School of Energy and Environmental Engineering, University of Science and Technology Beijing, Beijing 100083, China
[b] School of Chemistry and Biological Engineering, University of Science and Technology Beijing, Beijing 100083, China
[c] Beijing Engineering Research Center of Energy Saving and Environmental Protection, Beijing 100083, China
[d] Beijing Key Laboratory for Energy Saving and Emission Reduction of Metallurgical Industry, Beijing 100083, China

HIGHLIGHTS

- Microalgal biofilm structures formed under different light conditions are different.
- Biofilm formed under white light is heterogeneous with many voids.
- Biofilms formed under red and blue lights are homogeneous with low porosity.
- Biofilms formed under different photoperiods are different.
- Biofilm structures under different lights is interpreted by cell–cell interaction.

GRAPHICAL ABSTRACT

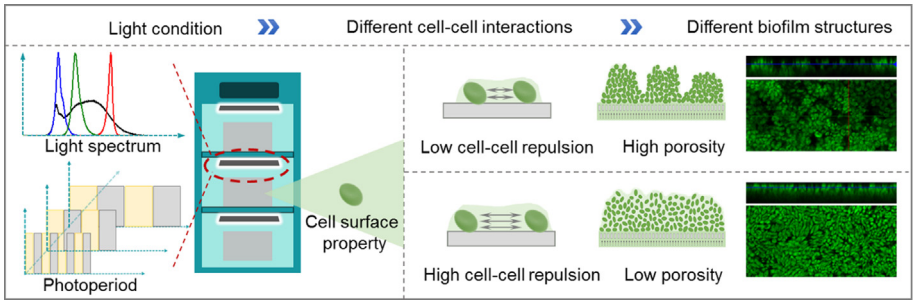

ARTICLE INFO

Article history:
Received 13 December 2019
Revised 7 September 2020
Accepted 15 September 2020
Available online 25 September 2020

Keywords:
Microalgae
Light spectrum
Photoperiod
Biofilm structure
Cell–cell interaction

ABSTRACT

Biofilm structure plays an important role in microalgae biofilm-based culture. This work aims to understand microalgal biofilm structures formed under different light conditions. Here, *Scenedesmus obliquus* was biofilm cultured under the light spectra of white, blue, green, and red, and the photoperiods of 5:5 s, 30:30 min, and 12:12 h (light : dark period). Biofilms were observed with confocal laser scanning microscopes and profilometry, then the porosity and roughness of biofilm were determined. We found that cells under white light formed a heterogeneous biofilm with many voids, high porosity, and roughness. While under red and blue lights, cells formed homogeneous biofilms with low porosity. Biofilm structures formed under different photoperiods were different. The mechanism of forming different biofilm structures under different light conditions was interpreted from the aspect of cell–cell interactions. Moreover, the results revealed that biomass accumulation increased with the increasing biofilm porosity due to the high effective diffusion coefficient.

1. Introduction

Microalgae have been considered as one of the promising biological sources to produce biofuels, high-value biomolecules and feeds, due to their fast growth rate, low nutrient requirements, and high lipid contents [1–5]. However, presently, the costs of microalgae-based commodities are still relatively high, which hinders their widespread commercialization [6–8]. Over the past few years, some researchers have reported that cultivating microalgae as biofilm (*i.e.*, cells are attached to a solid surface) can enhance the economic feasibility of microalgae-based biorefineries, owing to its higher harvesting efficiency, lower water consumption, and energy

* Corresponding author at: School of Energy and Environmental Engineering, University of Science and Technology Beijing, Beijing 100083, China.
E-mail address: xinruzhang@ustb.edu.cn (X. Zhang).

https://doi.org/10.1016/j.jcis.2020.09.057
0021-9797/

requirements, compared with suspended systems [9,10]. Therefore, microalgae biofilm-based systems have attracted much interest in recent years [11–13].

In this regard, many studies have indicated that the performance of microalgae biofilm cultivation can be affected by many factors [14,15], including (1) cultivation parameters (*e.g.*, light conditions, CO_2 supplement, nutrient concentration and sources, temperature, and pH), (2) cell properties (*e.g.*, cell surface hydrophobicity, production of extracellular polymeric substances, and species interactions), (3) characteristics of attachment materials (*e.g.*, surface microstructure, surface free energy, and surface electrical potential), (4) biofilm structure properties (*e.g.*, biofilm roughness, thickness, and porosity). Among these factors, biofilm structure can directly influence the transport of nutrient, light, and gas (*e.g.*, CO_2 and O_2), thus plays an important role in microalgae biofilm growth.

To date, extensive studies have studied biofilm structures formed under different hydrodynamics, temperatures, carbon sources, and nutrient concentrations [16,17]. However, most of these studies focused on bacterial biofilm structures [18–22]. For example, Cherifi et al. reported that nutrient concentration affected *L. monocytogenes* biofilm structures and the proportion of dead cells in biofilms [17]. Hartmann et al. found that the biofilm structure of the active *Vibrio cholerae* communities can be modulated by regulating the production of particular matrix components [18]. Shukla et al. found that the concentrations of Ca^{2+} influenced the microstructure and topography of *S. aureus* biofilm [23].

Fundamentally, microalgae, as a kind of photosynthetic microorganism, are different from bacteria, and they need light and CO_2 to perform photosynthesis [24,25]. Recently, for microalgae biofilms, some researchers found that the hollow biofilm structure was critical for light transmission in biofilm [26]. Meanwhile, the infiltration of O_2 and CO_2, and the permeability coefficient of biofilm can also be influenced by the biofilm structure[27,28]. These studies indicated that understanding the microalgal biofilm structure is of great significance for analyzing the transport phenomena in biofilms and improving the efficiency of biofilm-based microalgae cultivation systems. However, to date, little research has studied microalgal biofilm structures formed under different conditions.

To address this gap, this work explored the microalgae (*Scenedesmus obliquus*) biofilm structures formed under different light conditions, including the light spectra of white, blue, green, and red, and the photoperiods of 5:5 s, 30:30 min and 12:12 h (light: dark period). The biofilms were characterized by confocal laser scanning microscopes and profilometry via determining their porosity and roughness. The mechanism of forming different biofilm structures under different light conditions was analyzed from the aspect of cell–cell interactions via measuring the cell's surface properties. The study has significant implications for understanding the biofilm structure formed under different light conditions and analyzing the transport phenomena in biofilm.

2. Material and methods

2.1. Microalgae biofilm cultivation

The *Scenedesmus obliquus* (FACHB–276), which has great potential as biological sources to produce biofuels and high-value biomolecules, was used in this work [29]. Note that, before biofilm cultivation, *S. obliquus* was pre-cultivated in 500 mL flasks with 100 mL inoculum at 25 ± 1 °C under continuous irradiance of 100 μmol photons m^{-2} s^{-1} for 7 days in a rotary shaker at 120 rpm (ZWY-1102C, Labwit, China). After that, the pre-prepared homogeneous cell suspensions were evenly vacuum filtered onto some filtration membranes (served as attachment material for microalgal biofilm growth, diameter 50 mm, pore size 2 μm) to form microalgae biofilms with an initial inoculum density of 5.0 ± 0.1 g m^{-2}. Then, these filter membranes were attached to the prepared solidified BG–11 culture medium to maintain microalgae growth. The details can be found in supporting information (SI, Fig. S1, Table S1, Table S2). Fig. 1 shows the schematic of the experimental setup to culture microalgal biofilms under different light conditions. The biofilms were cultivated in polymethyl methacrylate chambers (400 × 200 × 200 mm), which were placed into an incubator, where the temperature was controlled at 25 ± 1 °C, as shown in Fig. 1(a, b) [30]. The compressed air enriched with 1% CO_2 (v/v) was aerated into the bioreactor with a constant flow rate of 0.1 VVM (volume of air per volume of culture per minute).

In the study, microalgae biofilms were cultivated under the light spectra of white, blue, green, and red, and the photoperiods of 5:5 s, 30:30 min, and 12:12 h. The white, blue, green, and red lights were provided by four kinds of light-emitting diodes (LEDs) (JK-W300200, JK-B300200, JK-G300200 and JK-R300200, J&K Photoelectric Technology, China). Fig. 1(c) shows the light spectra of these four LEDs characterized by a fiber spectrometer (USB4000, Ocean Optics Inc., USA). The photon flux densities of these four LEDs at biofilm surfaces were measured with a 4π quantum scalar sensor (QSL 2100, Biospherical Instruments, Inc, USA), and set to be ~100 μmol photons m^{-2} s^{-1}. The photoperiods of 5:5 s, 30:30 min, and 12:12 h were provided by connecting the white LED to a digital time relay, as shown in Fig. 1(d), and the photon flux densities of LEDs at biofilm surfaces were set to be ~200 μmol photons m^{-2} s^{-1} to maintain the same total amount of light as the other four light spectra regimes.

2.2. Characterization of biofilm: Microstructure and biomass

The microalgal biofilm microstructure and biomass were determined after 7 days of cultivation. Biofilm structure was observed with a confocal laser scanning microscope (Zeiss LSM780, Jena, Germany). Biofilm porosity (*P*) (see S4 in SI) was determined through the binarization of images with Image J software (version 1.51j8) [31,32] and calculated as follows:

$$P = A_P/A_t \quad (1)$$

where A_P is the pore area. A_t is the total area of each image.

The 3-dimensional surface architecture of microalgal biofilm was observed with the profilometric measurement using a laser scanning microscope (Olympus LEXT OLS 4000, Japan). Biofilm roughness was then determined from the 3-dimensional images. Note that the biofilm microstructure observation and biofilm surface architecture characterization were both conducted for three microalgae biofilm samples (see Fig. S3 in SI). At least five random fields of view were obtained for each sample. The biofilm images shown in this work were the representative images obtained in the measurements.

The biomass yield of microalgae biofilm was also determined after culturing for 7 days. In detail, the obtained microalgae biofilm was resuspended with deionized water to remove the soluble nutrients, followed by centrifuging and drying to a constant weight at 105 °C. After cooling in a desiccator, the microalgae biomass was weighed on an analytical balance (XS105, METTLER TOLEDO, Switzerland). All experiments were repeated at least three times. The results shown are mean ± standard deviation.

2.3. Measurement of microalgal cell properties

After 7 days of biofilm cultivation, microalgae cells were harvested to determine their properties, including cell morphology,

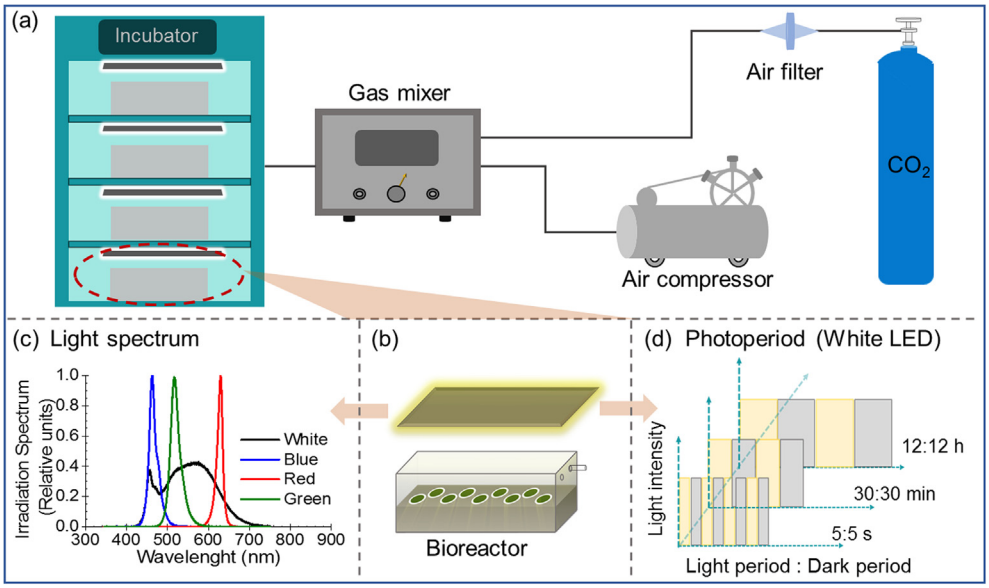

Fig. 1. Schematic of the experimental setup. (a) The biofilm cultivating bioreactor was placed into an incubator to maintain a proper temperature (25 ± 1 °C) for microalgae. The inside of the bioreactor was aerated with compressed air enriched with 1% CO_2 (v/v). (b) The microalgae biofilm cultivating bioreactor. (c) The light spectra of LEDs used in the experiment were white, blue, green, and red. (d) The photoperiods (light period: dark period) used in the experiment were 5:5 s, 30:30 min, and 12:12 h under white light. (For interpretation of the references to colour in this figure legend, the reader is referred to the web version of this article.)

contact angle, and surface free energy (SFE) components. Before the characterization, the microalgae cells were collected by resuspending microalgae biofilm into the phosphate buffer solution, followed by centrifugation at 1770 *g* for 4 min to remove cell debris. After that, the cell shape and size were determined by microscopy (BX61, Olympus, Japan). The contact angle was measured by a low-rate dynamic contact angle measurement on the prepared cell lawns using ultrapure water, formamide, and methylene iodide as the probe liquids [33,34]. The details can be found in S5.1. The SFE components of microalgae cells, including total SFE (γ^{tot}), Lifshitz-van der Waals (LW) component of SFE (γ^{LW}), electron acceptor component of SFE (γ^{+}), and electron donor component of SFE (γ^{-}) were determined based on the contact angle measurements in conjunction with the Lifshitz-van der Waals–Lewis acid-base (LW–AB) approach (see SI S5.2) [35,36].

2.4. Statistical analysis

The measured data of the biofilm porosity, roughness, and cell surface properties were analyzed using MATLAB (9.6 MathWorks, USA) software. One-way ANOVA was performed to study the significance of cell surface properties and biofilm structures formed under different light conditions (see S5.3, S6, and S7). The *P*-values less than 0.05 were considered to be statically significant. The results shown are mean ± 95% confidence intervals.

3. Results and discussion

3.1. Biofilm structure

To understand biofilm structures formed under different light conditions, the *S. obliquus* biofilms were observed with a confocal laser scanning microscope. Fig. 2(a1–a7) show the representative confocal laser scanning images of biofilms formed under the white, blue, green, and red lights, and the photoperiods of 5:5 s, 30:30 min, and 12:12 h, respectively, which indicated that the microstructures of these biofilms had great differences. In particular, Fig. 2(a1, a3, a7) indicate that the biofilms formed under the white and green lights, and the photoperiod of 12:12 h were more heterogeneous and had more open voids with a diameter ranging from 50~100 μm, compared with those formed under other light conditions. Alternatively, Fig. 2(a2, a4, a6) show that the biofilms formed under the blue and red lights, and the photoperiod of 30:30 min had homogenous microstructure and no obvious large voids.

Based on the laser confocal images, the biofilm porosity was calculated by ImageJ software. As shown in Fig. 2(a8), the determined porosity for biofilms formed under the white, blue, green and red lights, and the photoperiods of 5:5 s, 30:30 min, and 12:12 h were 41.98 ± 1.36, 29.36 ± 1.64, 35.97 ± 2.18, 29.65 ± 1.44, 32.27 ± 2.26, 30.12 ± 1.20 and 37.67 ± 2.25%, respectively. Based on the statistical analysis (see SI S6), we think that the porosities of biofilms formed under different light conditions were significantly different ($p \leq 0.05$). The results indicated that the biofilms with heterogeneous structures and large open voids exhibited high biofilm porosity, while the biofilms with homogenous structures presented low biofilm porosity.

Furthermore, Fig. 2(b1–b7) show the representative 3-dimensional images for the microalgae biofilms formed under the white, blue, green, and red lights, and the photoperiods of 5:5 s, 30:30 min, and 12:12 h, respectively. Fig. 2(b8) shows the determined roughness for these biofilms. The results suggested that the surface roughness of these biofilms was different, and the biofilms with heterogeneous structures (*e.g.*, white light and the photoperiods of 12:12 h) generally had high biofilm roughness, whereas, the biofilms with homogeneous structures (*e.g.*, blue and red lights) exhibited low biofilm roughness.

These above results indicated that biofilm structures formed under different light conditions were different. Microalgal biofilms formed under the white light and the photoperiods of 12:12 h were heterogeneous with many voids, and had high biofilm porosity and roughness. Whereas, the biofilms formed under blue and red lights were homogenous, and had low biofilm porosity and roughness.

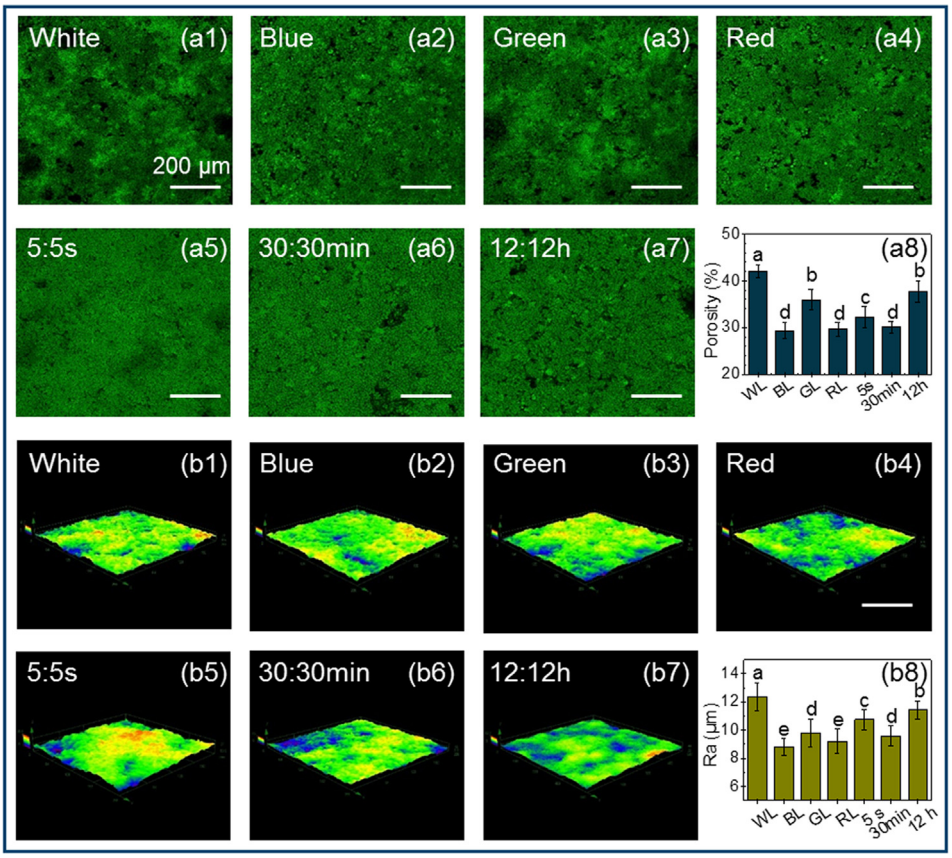

Fig. 2. (a1–a7) The microstructures of *S. obliquus* biofilms formed under the white, blue, green, and red lights, and the photoperiods of 5:5 s, 30:30 min, and 12:12 h under white light, respectively. (a8) The determined porosity of biofilm formed under different light conditions. (b1–b7) The 3-dimensional images of *S. obliquus* biofilms formed under the white, blue, green, and red lights, and the photoperiods of 5:5 s, 30:30 min, and 12:12 h under white light, respectively. (b8) The measured roughness of biofilm formed under different light conditions. (For interpretation of the references to colour in this figure legend, the reader is referred to the web version of this article.)

3.2. Analyzing the biofilm structure from the aspect of cell–cell interaction

Our recent study found that the microalgae biofilms cultured under different conditions exhibited different cell surface compositions and chemical groups. [37,38] Predictably, the alteration of cell surface compositions and chemical groups can lead to the variation of cell SFE, and change the cell–cell interactions accordingly. Based on the thermodynamics, biofilm structure can be affected by cell–cell interactions. Generally, cell–cell interaction could be evaluated by co-adhesion energy ($\Delta G_{\text{co-adh}}$) [39–41], which represents the free energy change before and after co-adhesion. Therefore, from a free energy point of view, a high $\Delta G_{\text{co-adh}}$ means co-adhesion would be unfavorable, and cells with high $\Delta G_{\text{co-adh}}$ would have a high cell–cell repulsive interaction. Whereas, a low $\Delta G_{\text{co-adh}}$ leads to co-adhesion, and cells with low $\Delta G_{\text{co-adh}}$ would have a low cell–cell repulsive interaction (or a high attractive interaction). The $\Delta G_{\text{co-adh}}$ can be expressed as [39,42],

$$\Delta G_{\text{co}-\text{adh}} = \Delta G^{\text{LW}}_{\text{co}-\text{adh}} + \Delta G^{\text{AB}}_{\text{co}-\text{adh}} \tag{2}$$

where $\Delta G^{\text{LW}}_{\text{co}-\text{adh}}$ is the LW component of co-adhesion energy, and $\Delta G^{\text{AB}}_{\text{co}-\text{adh}}$ is the AB component of co-adhesion energy. $\Delta G^{\text{LW}}_{\text{co}-\text{adh}}$ and $\Delta G^{\text{AB}}_{\text{co}-\text{adh}}$ can be expressed as,

$$\Delta G^{\text{LW}}_{\text{co}-\text{adh}} = -2\left(\sqrt{\gamma^{\text{LW}}_{\text{mv}}} - \sqrt{\gamma^{\text{LW}}_{\text{lv}}}\right)^2 \tag{3}$$

$$\Delta G^{\text{AB}}_{\text{co}-\text{adh}} = -4\left(\sqrt{\gamma^{+}_{\text{mv}}} - \sqrt{\gamma^{+}_{\text{lv}}}\right) \times \left(\sqrt{\gamma^{-}_{\text{mv}}} - \sqrt{\gamma^{-}_{\text{lv}}}\right) \tag{4}$$

where $\gamma^{\text{LW}}_{\text{mv}}$ and $\gamma^{\text{LW}}_{\text{lv}}$ are the LW components of SFE for microalgae–vapor and liquid–vapor interactions, respectively. γ^{+}_{mv} and γ^{+}_{lv} are the electron acceptor components of SFEs for microalgae–vapor and liquid–vapor interactions, respectively, and γ^{-}_{mv} and γ^{-}_{lv} are the electron donor components of SFEs for these interactions. Substituting Eqs. (3) and (4) into Eq. (2) yields,

$$\Delta G_{\text{co}-\text{adh}} = -2\left(\sqrt{\gamma^{\text{LW}}_{\text{mv}}} - \sqrt{\gamma^{\text{LW}}_{\text{lv}}}\right)^2 - 4\left(\sqrt{\gamma^{+}_{\text{mv}}} - \sqrt{\gamma^{+}_{\text{lv}}}\right) \times \left(\sqrt{\gamma^{-}_{\text{mv}}} - \sqrt{\gamma^{-}_{\text{lv}}}\right) \tag{5}$$

Evidently, Eq. (5) indicates that the surface properties of cells and liquid medium significantly influence the $\Delta G_{\text{co-adh}}$, thus the cell–cell interactions.

Therefore, we characterized the cell's properties, including size, contact angle, and SFE for the *S. obliquus* cells cultured under different light conditions. Table 1 shows the size and SFEs of these microalgae. It was found that the cell sizes were almost the same, indicating that the culture condition had less influence on cell size. Table S3 shows the contact angles of water (θ^{W}), formamide (θ^{F}), and methylene iodide (θ^{M}) on microalgal cell lawns. The results indicated that θ^{W} on cells cultured under different light conditions ranged from 26.9 ± 3.7° to 43.6 ± 4.7°, indicating that all these cells were hydrophilic, which agreed well with the literature [43,44]. Table 1 shows the SFEs components for cells determined by the LW–AB approach, *i.e.*, $\gamma^{\text{tot}}_{\text{mv}}$, $\gamma^{\text{LW}}_{\text{mv}}$, γ^{+}_{mv} and γ^{-}_{mv}. The results demonstrated that the γ^{tot} of these cells ranged from 47.09 to 51.89 mJ/m^2, and the cells all had weak electron acceptors (γ^{+}) ranging from ~1.26 mJ/m^2 to ~2.48 mJ/m^2, which agreed well with

Table 1
The size and SFE components of *S. obliquus* cells cultured under different light conditions.

Light conditions	Length (L)	Width (W)	L/W	γ^{tot}	γ^{LW}	γ^{+}	γ^{-}
	(μm)			(mJ/m^2)			
White	8.0 ± 2.5	3.7 ± 1.3	2.1	48.5 ± 1.1	30.9 ± 1.0	2.3 ± 0.6	33.2 ± 4.4
Blue	7.9 ± 1.7	3.5 ± 0.9	2.2	49.4 ± 1.3	30.4 ± 1.1	1.7 ± 0.4	52.2 ± 3.5
Green	9.3 ± 2.3	4.4 ± 1.3	2.1	47.2 ± 2.2	31.3 ± 1.1	1.4 ± 0.6	46.0 ± 4.4
Red	10.4 ± 2.4	4.1 ± 0.9	2.5	47.1 ± 2.4	31.5 ± 0.7	1.3 ± 0.5	48.1 ± 4.9
5:5 s	9.8 ± 1.9	4.4 ± 1.2	2.2	50.3 ± 1.1	31.6 ± 1.3	2.0 ± 0.5	43.5 ± 3.2
30:30 min	8.8 ± 2.1	4.2 ± 1.4	2.1	51.9 ± 1.3	31.4 ± 1.6	2.3 ± 0.6	46.7 ± 4.2
12:12 h	7.9 ± 2.2	3.7 ± 1.1	2.1	49.9 ± 1.2	28.9 ± 1.2	2.5 ± 0.5	44.3 ± 3.3

the literature [36,38]. Whereas, the cells exhibited high values of electron donor characters (γ^-), ranging from 33 to 53 mJ/m^2, which indicated that γ^- of cells can be significantly affected by light conditions.

Furthermore, based on these cell surface properties, $\Delta G_{co\text{-}adh}$ were determined. Fig. 3 shows that $\Delta G_{co\text{-}adh}$ for microalgal cells cultured under the white, blue, green, and red lights, and the photoperiods of 5:5 s, 30:30 min, and 12:12 h were 8.1 ± 5.7, 31.9 ± 4.5, 21.7 ± 6.2, 29.0 ± 7.0, 20.6 ± 4.2, 23.0 ± 5.2 and 20.9 ± 4.1 mJ/m^2, respectively. The statistical analysis (see SI S7) revealed that the cell–cell interactions in biofilm under different light conditions were significantly different ($P \leq 0.05$). Based on the physical meaning of $\Delta G_{co\text{-}adh}$, the cells with low $\Delta G_{co\text{-}adh}$ (*e.g.*, cells cultured under white light) would prefer to form co-adhesion, due to the low cell–cell repulsive interactions, as shown by the insets in Fig. 3. Whereas, the cells with high $\Delta G_{co\text{-}adh}$ (*e.g.*, cells cultured under blue and red lights) would be difficult to form co-adhesion, due to the high cell–cell repulsive interactions.

Predictably, as shown in Fig. 4(a), the cells with low cell–cell repulsive interaction (*i.e.*, low $\Delta G_{co\text{-}adh}$) would prefer to form high cell aggregations, which can make biofilm more heterogeneous, and significantly increase the biofilm porosity and roughness. Meanwhile, Fig. 4(b) indicates that the cells with high cell–cell repulsive interaction (*i.e.*, high $\Delta G_{co\text{-}adh}$) would disperse well in the liquid medium, making the biofilm more homogenous, which can decrease the biofilm porosity and roughness. Fig. 4(c) shows the biofilm porosity and roughness as a function of $\Delta G_{co\text{-}adh}$ for the cells cultured under different light conditions. The results indicated that the porosity and roughness of biofilm decreased with the increasing $\Delta G_{co\text{-}adh}$, owing to the increasing cell–cell repulsive interactions.

These above results demonstrated that biofilm structures formed under different light conditions could be interpreted by analyzing the cell–cell interactions via determining the cell's physicochemical properties. Owing to the low cell–cell repulsive interaction and low $\Delta G_{co\text{-}adh}$, the cells cultured under white light and the photoperiods of 12:12 h would form a heterogeneous biofilm, with many voids, high biofilm porosity, and high roughness.

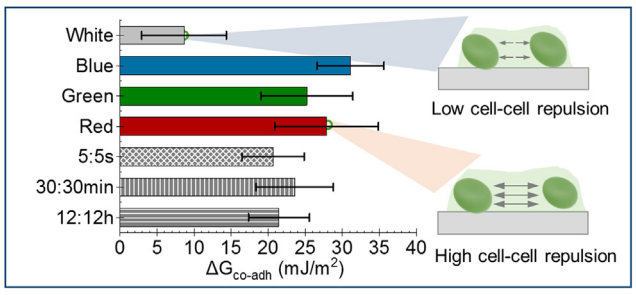

Fig. 3. The co-adhesion energy ($\Delta G_{co\text{-}adh}$) of *S. obliquus* cells cultured under different light conditions.

Whereas, owing to the high cell–cell repulsive interaction and high $\Delta G_{co\text{-}adh}$, the cells cultured under blue and red lights would form a homogenous biofilm, with low biofilm porosity and roughness. However, it should be noted that the low porosity of microalgae biofilms formed under red or blue lights might also be related to the self-adaption phenomena of biofilm for reducing the light transfer into the biofilms due to the variation in the physiological properties of cells (*i.e.*, photosynthesis performance, oxidative stress, *etc.*). [45,46] Further studies need to be conducted to draw more definite conclusions.

3.3. Effects of biofilm structure on the biomass of *S. obliquus* biofilm

The above results indicated that light conditions could influence the biofilm structures of *S. obliquus*, the biofilm porosity as well as roughness. Fundamentally, biofilm structure can directly affect the transport phenomena of nutrient, light, and gas (*e.g.*, CO_2 and O_2) in the biofilm, and may influence microalgae biofilm growth as well as biomass accumulation. Particularly, in this study, because the bioreactor is an evaporation-driven porous substrate bioreactor [27,30], in which nutrients and gas are transported in cell aggregates of biofilms predominately by diffusion. Based on the literature, the diffusion rate of nutrients in the biofilm can be evaluated by the effective diffusion coefficient (D_e), which can be expressed as [27,47]:

$$D_e = D \cdot \frac{P}{\tau} \tag{6}$$

where P is the biofilm porosity, D represents the diffusion coefficient in liquid medium (*i.e.*, water), and τ is the tortuosity of the biofilm.

Based on the Eq. (6), it can be found that the diffusion of nutrients is positively correlated with the biofilm porosity. In this regard, some researchers have studied the influence of biofilm porosity on mass transfer phenomena in biofilm. For example, Cai et al. analyzed the internal mass distribution in the microbial fuel cell, and reported that, for the biofilm with higher porosity, the mass transfer would be much easier, and the transfer resistance would decrease [48]. By studying the effect of biofilm structural deformation on hydraulic resistance, Jafari et al. found that the higher biofilm porosity was beneficial to biofilm permeability [49]. Meanwhile, using the nuclear magnetic resonance method, Renslow et al. studied the effective diffusion coefficient in the live-cell biofilms, and indicated that the diffusion increased in the presence of biofilm voids [50]. These studies suggested that the hollow biofilm structure may promote the effective diffusion of nutrients in biofilm.

Furthermore, predictably, the increasing diffusion of nutrients may promote biofilm growth, thus increase biomass accumulation. Therefore, we measured the biomass cultured under different light conditions. As shown by Fig. S4, the biomass under different light conditions ranged from approximately 43 to 49 g/m^2. Furthermore, we analyzed the relationship between the biomass under different

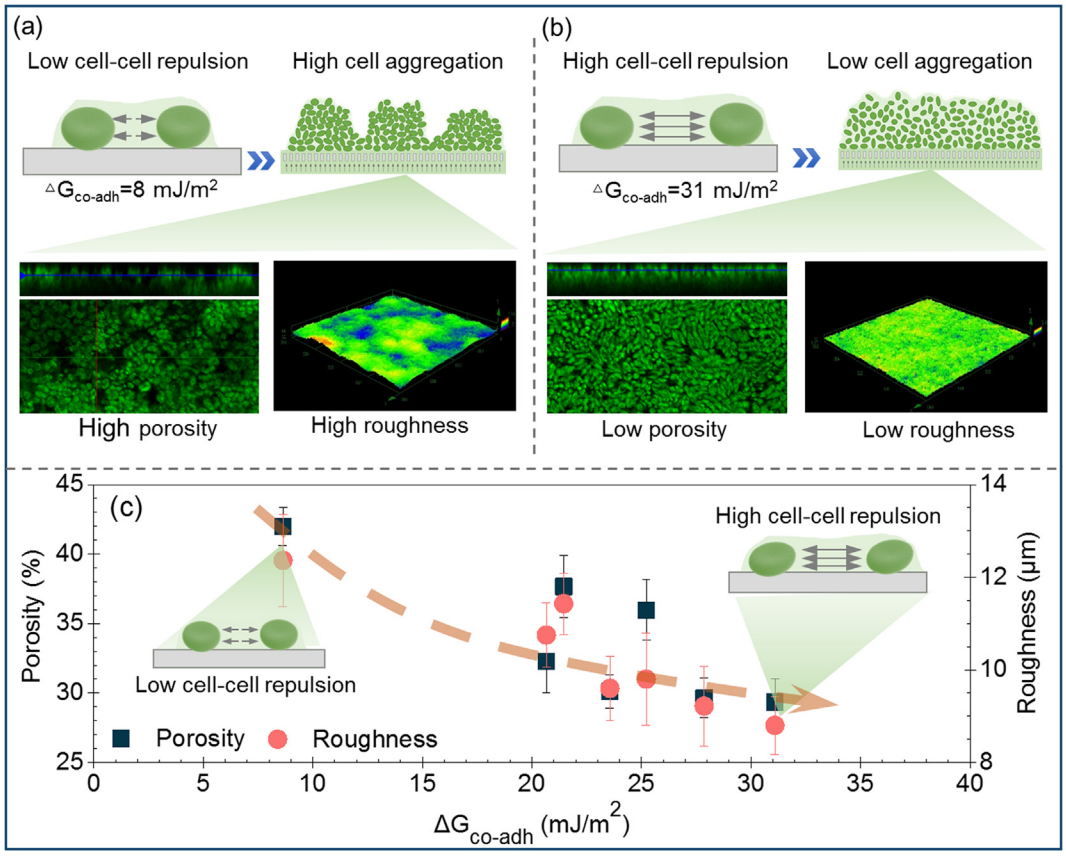

Fig. 4. (a, b) Schematic to illustrate the mechanism of forming different biofilm structures under different light conditions from the aspect of the cell–cell interaction. Microalgae cells with low cell–cell repulsion would form a heterogeneous biofilm with many voids and high porosity. Microalgae cells with high cell–cell repulsion would form a flat and homogeneous biofilm with low porosity and roughness. (c) The biofilm porosity and biofilm roughness as a function of $\Delta G_{co\text{-}adh}$ for cells cultured under different light conditions.

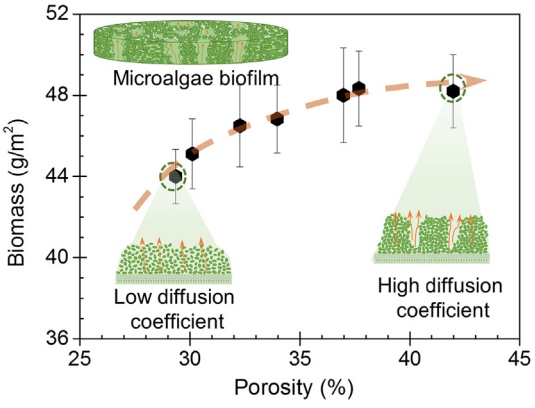

Fig. 5. The biofilm biomass as a function of biofilm porosity.

light conditions and biofilm porosity. Fig. 5 revealed that the biomass accumulation increased with increasing biofilm porosity, but the speed of increase became slower gradually. As shown by the insets in Fig. 5, because a homogenous biofilm exhibited a low porosity and a low diffusion coefficient in biofilm, while a heterogeneous biofilm possessed a high porosity and a high diffusion coefficient, this means that the nutrient transport in heterogeneous biofilm with high porosity would be much easier than that in homogenous biofilm with low porosity. In addition, the heterogeneous biofilm with high porosity would also facilitate the radiation of external light and the transfer of O_2 and CO_2 in biofilm, which are conducive to the cells photosynthesis. Therefore, we think that the increasing transport of nutrient, light, O_2 and CO_2 in heterogeneous biofilms with high porosity may be the reason for their increasing biomass.

Moreover, it should be noted that our results indicated that the biomass yields of microalgae biofilm cultured under blue or red lights were lower than those under white or green lights, which may be due to the less porous biofilm structures (with low diffusion coefficient in biofilm). Meanwhile, Mooij et al. [51] found that the biomass of *Chlamydomonas reinhardtii* under blue or red light was also lower than that under sunlight or warm white light, which may be due to the cell's insufficient utilization of high energy generated by blue and red lights. These studies revealed that the effects of light conditions on the microalgae growth were very complex. Further studies should be conducted for more definite conclusions. Nevertheless, we think that the results of this study would have important implications for understanding the biofilm structures formed under different light conditions and selecting the suitable light regime in microalgae biofilm-based cultivation systems.

4. Conclusion

Several previous studies reported that biofilm structures could be affected by the hydrodynamics, temperatures, nutrient supply, and the secretion of extracellular polymeric substance [16–18,37]. The study innovatively found that light conditions (white, blue, green, and red lights, and the photoperiods of 5:5 s, 30:30 min, and 12:12 h) could influence *S. obliquus* biofilm struc-

tures, porosity, and roughness. The mechanism of forming different biofilm structures under these light conditions can be interpreted from the aspect of cell–cell interactions. We revealed that due to the low cell–cell repulsive interaction and low $\Delta G_{co\text{-}adh}$, *S. obliquus* cells cultured under white light and the photoperiods of 12:12 h formed heterogeneous biofilm with many voids, higher biofilm porosity (~42%) and roughness. Whereas, due to the high cell–cell repulsive interaction and high $\Delta G_{co\text{-}adh}$, the cells under blue and red lights formed homogenous biofilm with lower biofilm porosity (~30%) and roughness. Furthermore, the results indicated that the biomass of *S. obliquus* biofilms cultured under these light conditions increased with the increasing biofilm porosity. This may be because the heterogeneous biofilm with high porosity would facilitate the transport of nutrient, light, O_2 and CO_2 in biofilms [27,28]. The study has important implications for understanding the microalgal biofilm structures formed under different culture conditions. It should be noted that this work only studied the biofilm structures formed under some typical light spectra and photoperiods, the biofilm structures formed under other culture conditions (such as light intensity, CO_2 supply, nutrient concentrations, *etc.*) should also be conducted in further studies.

CRediT authorship contribution statement

Hao Yuan: Investigation, Methodology, Data curation, Formal analysis, Software, Writing - original draft, Writing - review & editing. **Yi Wang:** Investigation, Methodology, Data curation, Writing - review & editing. **Zhijian Lai:** Investigation, Methodology, Data curation. **Xinru Zhang:** Conceptualization, Data curation, Funding acquisition, Formal analysis, Investigation, Methodology, Resources, Supervision, Validation, Writing - original draft, Writing - review & editing. **Zeyi Jiang:** Investigation, Methodology, Supervision, Writing - review & editing. **Xinxin Zhang:** Conceptualization, Investigation, Supervision, Writing - review & editing.

Declaration of Competing Interest

The authors declare that they have no known competing financial interests or personal relationships that could have appeared to influence the work reported in this paper.

Acknowledgments

This work is supported by the National Natural Science Foundation of China (No. 51706019), and the Fundamental Research Funds for the Central Universities (No. FRF-BD-20-09A, FRF–AS–17–001 and No. FRF–BD–18–015A).

Appendix A. Supplementary material

Supplementary data to this article can be found online at https://doi.org/10.1016/j.jcis.2020.09.057.

References

[1] W. Zhou, J. Wang, P. Chen, C. Ji, Q. Kang, B. Lu, K. Li, J. Liu, R. Ruan, Bio-mitigation of carbon dioxide using microalgal systems: Advances and perspectives, Renew. Sustain. Energy Rev. 76 (2017) 1163–1175.
[2] P. Chen, Q. Xie, M. Addy, W. Zhou, Y. Liu, Y. Wang, Y. Cheng, K. Li, R. Ruan, Utilization of municipal solid and liquid wastes for bioenergy and bioproducts production, Bioresour. Technol. 215 (2016) 163–172.
[3] S.R. Chia, H.C. Ong, K.W. Chew, P.L. Show, S.-M. Phang, T.C. Ling, D. Nagarajan, D.-J. Lee, J.-S. Chang, Sustainable approaches for algae utilisation in bioenergy production, Renewable Energy 129 (2018) 838–852.
[4] S. Gupta, S.B. Pawar, R.A. Pandey, Current practices and challenges in using microalgae for treatment of nutrient rich wastewater from agro-based industries, Sci. Total Environ. 687 (2019) 1107–1126.
[5] L.-P. Guo, Y. Zhang, W.-C. Li, Sustainable microalgae for the simultaneous synthesis of carbon quantum dots for cellular imaging and porous carbon for CO2 capture, J. Colloid Interf. Sci. 493 (2017) 257–264.
[6] A. Mantzorou, F. Ververidis, Microalgal biofilms: A further step over current microalgal cultivation techniques, Sci. Total Environ. 651 (2019) 3187–3201.
[7] N. Uduman, Y. Qi, M.K. Danquah, G.M. Forde, A. Hoadley, Dewatering of microalgal cultures: A major bottleneck to algae-based fuels, J. Renewable Sustainable Energy 2 (1) (2010) 23–571.
[8] G. De Bhowmick, A.K. Sarmah, R. Sen, Zero-waste algal biorefinery for bioenergy and biochar: A green leap towards achieving energy and environmental sustainability, Sci. Total Environ. 650 (2019) 2467–2482.
[9] F. Berner, K. Heimann, M. Sheehan, Microalgal biofilms for biomass production, J. Appl. Phycol. 27 (5) (2015) 1793–1804.
[10] D. Hoh, S. Watson, E. Kan, Algal biofilm reactors for integrated wastewater treatment and biofuel production: A review, Chem. Eng. J. 287 (2016) 466–473.
[11] Y. Zheng, Y. Huang, A. Xia, F. Qian, C. Wei, A rapid inoculation method for microalgae biofilm cultivation based on microalgae-microalgae co-flocculation and zeta-potential adjustment, Bioresour. Technol. (2019).
[12] L.-L. Zhuang, D. Yu, J. Zhang, F.-F. Liu, Y.-H. Wu, T.-Y. Zhang, G.-H. Dao, H.-Y. Hu, The characteristics and influencing factors of the attached microalgae cultivation: A review, Renew. Sustain. Energy Rev. 94 (2018) 1110–1119.
[13] X. Zhao, K. Kumar, M.A. Gross, T.E. Kunetz, Z. Wen, Evaluation of revolving algae biofilm reactors for nutrients and metals removal from sludge thickening supernatant in a municipal wastewater treatment facility, Water Res. 143 (2018) 467–478.
[14] J. Wang, W. Liu, T. Liu, Biofilm based attached cultivation technology for microalgal biorefineries—A review, Bioresour. Technol. 244 (2017) 1245–1253.
[15] P.J. Schnurr, D.G. Allen, Factors affecting algae biofilm growth and lipid production: A review, Renew. Sustain. Energy Rev. 52 (2015) 418–429.
[16] D. Langenbach, M. Melkonian, Optimising biomass and peridinin accumulation in the dinoflagellate Symbiodinium voratum using a twin-layer porous substrate bioreactor, J. Appl. Phycol. 31 (1) (2019) 21–28.
[17] T. Cherifi, M. Jacques, S. Quessy, P. Fravalo, Impact of nutrient restriction on the structure of listeria monocytogenes biofilm grown in a microfluidic system, Front. Microbiol. 8 (864) (2017).
[18] R. Hartmann, P.K. Singh, P. Pearce, R. Mok, B. Song, F. Díaz-Pascual, J. Dunkel, K. Drescher, Emergence of three-dimensional order and structure in growing biofilms, Nat. Phys. 15 (3) (2019) 251.
[19] L. Vidakovic, P.K. Singh, R. Hartmann, C.D. Nadell, K. Drescher, Dynamic biofilm architecture confers individual and collective mechanisms of viral protection, Nat. Microbiol. 3 (1) (2018) 26–31.
[20] L. Tan, F. Zhao, Q. Han, A. Zhao, P.K. Malakar, H. Liu, Y. Pan, Y. Zhao, High correlation between structure development and chemical variation during biofilm formation by vibrio parahaemolyticus, Front. Microbiol. 9 (2018). 1881–1881.
[21] H. Cai, H. Fan, L. Zhao, H. Hong, L. Shen, Y. He, H. Lin, J. Chen, Effects of surface charge on interfacial interactions related to membrane fouling in a submerged membrane bioreactor based on thermodynamic analysis, J. Colloid Interf. Sci. 465 (2016) 33–41.
[22] A. Elbourne, J. Chapman, A. Gelmi, D. Cozzolino, R.J. Crawford, V.K. Truong, Bacterial-nanostructure interactions: The role of cell elasticity and adhesion forces, J. Colloid Interf. Sci. 546 (2019) 192–210.
[23] S.K. Shukla, T.S. Rao, Effect of calcium on Staphylococcus aureus biofilm architecture: a confocal laser scanning microscopic study, Colloids Surf., B 103 (2013) 448–454.
[24] H.-X. Chang, Y. Huang, Q. Fu, Q. Liao, X. Zhu, Kinetic characteristics and modeling of microalgae Chlorella vulgaris growth and CO2 biofixation considering the coupled effects of light intensity and dissolved inorganic carbon, Bioresour. Technol. 206 (2016) 231–238.
[25] P.J. Schnurr, O. Molenda, E. Edwards, G.S. Espie, D.G. Allen, Improved biomass productivity in algal biofilms through synergistic interactions between photon flux density and carbon dioxide concentration, Bioresour. Technol. 219 (2016) 72–79.
[26] T. Li, B. Piltz, B. Podola, A. Dron, D. de Beer, M. Melkonian, Microscale profiling of photosynthesis-related variables in a highly productive biofilm photobioreactor, Biotechnol. Bioeng. 113 (5) (2016) 1046–1055.
[27] T. Li, B. Podola, M. Melkonian, Investigating dynamic processes in a porous substrate biofilm photobioreactor — A modeling approach, Algal Research 13 (2016) 30–40.
[28] T.E. Murphy, E. Fleming, H. Berberoglu, Vascular structure design of an artificial tree for microbial cell cultivation and biofuel production, Transp. Porous Media 104 (1) (2014) 25–41.
[29] S. Ma, D. Li, Y. Yu, D. Li, R.S. Yadav, Y. Feng, Application of a microalga, Scenedesmus obliquus PF3, for the biological removal of nitric oxide (NO) and carbon dioxide, Environ. Pollut. 252 (2019) 344–351.
[30] X. Zhang, H. Yuan, L. Guan, X. Wang, Y. Wang, Z. Jiang, L. Cao, X. Zhang, Influence of photoperiods on microalgae biofilm: photosynthetic performance, biomass yield, and cellular composition, Energies 12 (19) (2019) 3724.
[31] A. Heydorn, A.T. Nielsen, M. Hentzer, C. Sternberg, M. Givskov, B.K. Ersbøll, S. Molin, Quantification of biofilm structures by the novel computer program COMSTAT, Microbiology 146 (10) (2000) 2395–2407.
[32] X. Yang, H. Beyenal, G. Harkin, Z. Lewandowski, Quantifying biofilm structure using image analysis, J. Microbiol. Methods 39 (2) (2000) 109–119.

[33] X. Zhang, X. Cai, K. Jin, Z. Jiang, H. Yuan, Y. Jia, Y. Wang, L. Cao, X. Zhang, Determining the surface tension of two-dimensional nanosheets by a low-rate advancing contact angle measurement, Langmuir 35 (25) (2019) 8308–8315.
[34] X. Zhang, H. Yuan, Z. Jiang, D. Lin, X. Zhang, Impact of surface tension of wastewater on biofilm formation of microalgae Chlorella sp, Bioresour. Technol. 266 (2018) 498–506.
[35] D.Y. Kwok, A.W. Neumann, Contact angle measurement and contact angle interpretation, Adv. Colloid Interface Sci. 81 (3) (1999) 167–249.
[36] P.K. Sharma, K. Hanumantha Rao, Analysis of different approaches for evaluation of surface energy of microbial cells by contact angle goniometry, Adv. Colloid Interface Sci. 98 (3) (2002) 341–463.
[37] X. Zhang, H. Yuan, Y. Wang, L. Guan, Z. Zeng, Z. Jiang, X. Zhang, Cell surface energy affects the structure of microalgal biofilm, Langmuir 36 (12) (2020) 3057–3063.
[38] H. Yuan, X. Zhang, Z. Jiang, X. Wang, X. Chen, L. Cao, X. Zhang, Analyzing the effect of pH on microalgae adhesion by identifying the dominant interaction between cell and surface, Colloids Surf., B 177 (2019) 479–486.
[39] R. Bos, H.C. van der Mei, H.J. Busscher, Physico-chemistry of Initial Microbial Adhesive Interactions – Its Mechanisms and Methods for Study, FEMS Microbiol. Rev. 23 (2) (1999) 179–230.
[40] A. Ozkan, H. Berberoglu, Cell to substratum and cell to cell interactions of microalgae, Colloids Surf., B 112 (2013) 302–309.
[41] G. Yu, X. Cai, L. Shen, J. Chen, H. Hong, H. Lin, R. Li, A novel integrated method for quantification of interfacial interactions between two rough bioparticles, J Colloid Interf Sci 516 (2018) 295–303.
[42] A. Stammitti-Scarpone, E.J. Acosta, Solid-liquid-liquid wettability and its prediction with surface free energy models, Adv. Colloid Interface Sci. 264 (2019) 28–46.
[43] H. Yuan, X. Zhang, Z. Jiang, X. Chen, X. Zhang, Quantitative criterion to predict cell adhesion by identifying dominant interaction between microorganisms and abiotic surfaces, Langmuir 35 (9) (2019) 3524–3533.
[44] A. Ozkan, H. Berberoglu, Physico-chemical surface properties of microalgae, Colloids Surf., B 112 (2013) 287–293.
[45] H. Yuan, X. Zhang, Z. Jiang, X. Wang, Y. Wang, L. Cao, X. Zhang, Effect of light spectra on microalgal biofilm: Cell growth, photosynthetic property, and main organic composition, Renewable Energy 157 (2020) 83–89.
[46] M. Gambino, F. Cappitelli, Mini-review: Biofilm responses to oxidative stress, Biofouling 32 (2) (2016) 167–178.
[47] H.L. Weissberg, Effective diffusion coefficient in porous media, J. Appl. Phys. 34 (9) (1963) 2636–2639.
[48] W.-F. Cai, J.-F. Geng, K.-B. Pu, Q. Ma, D.-W. Jing, Y.-H. Wang, Q.-Y. Chen, H. Liu, Investigation of a two-dimensional model on microbial fuel cell with different biofilm porosities and external resistances, Chem. Eng. J. 333 (2018) 572–582.
[49] M. Jafari, P. Desmond, M.C.M. van Loosdrecht, N. Derlon, E. Morgenroth, C. Picioreanu, Effect of biofilm structural deformation on hydraulic resistance during ultrafiltration: A numerical and experimental study, Water Res 145 (2018) 375–387.
[50] R.S. Renslow, P.D. Majors, J.S. McLean, J.K. Fredrickson, B. Ahmed, H. Beyenal, In situ effective diffusion coefficient profiles in live biofilms using pulsed-field gradient nuclear magnetic resonance, Biotechnol. Bioeng. 106 (6) (2010) 928–937.
[51] T. de Mooij, G. de Vries, C. Latsos, R.H. Wijffels, M. Janssen, Impact of light color on photobioreactor productivity, Algal Research 15 (2016) 32–42.